Evaluation of the Geometrical Properties Distribution Along the Human Ribs Using Different X-Ray Imaging Methods

Rafal Perz, Jacek Toczyski, Matt Kindig, Daisuke Ito, Susumu Ejima, Koichi Kamiji, Tsuyoshi Yasuki, Jeff Crandall, Damien Subit

Abstract This paper presents methods to investigate the dependence of the CT images resolution to the rib geometrical properties and the rib mechanical behavior during antero-posterior bending. This study suggests that clinical-CT images may be sufficient to create proper rib cage geometry.

PMHS ribs were harvested and tested under antero-posterior bending. After the tests, 34 rib slices were cut from the posterior, lateral and anterior aspects. The sections were imaged with micro- and clinical-CT, and their geometrical parameters were compared. The results showed that clinical-CT overestimates the overall cross-sectional area by around 8%, cortical area by 40% and moments of inertia by 50%. A numerical scheme was developed to correct the measurements obtained from the clinical-CT using the information gathered locally from micro-CT.

A parametric study was carried out: finite element models for the antero-posterior bending tests were created based on the variations in geometrical parameters defined from the CT analysis. It was found that the FE model's mechanical response was greatly sensitive to the image modality. The method presented in this study introduces a new approach that combines clinical-CT images with the local measurements from micro-CT. This combination was found to be effective in reducing the disparity between the experimental and numerical results.

Keywords: PMHS medical CT, resolution, ribs beam model, thorax

I. INTRODUCTION

One of the main causes of death during frontal car crashes is a thorax injury [1-2]. It is estimated that 70% of fatalities suffered thorax trauma and in 30% of those, chest injuries were the main cause of death [3]. In regard to societal harm, injuries to the chest rank in second place after injuries to the head [4].

The main methods to learn about human thorax behavior during intensive loading are the tabletop and sled track tests performed on Post Mortem Human Surrogates (PMHS) [5]. Among those methods the computational models of the human ribcage are commonly used to predict injuries such as rib fractures [6-10]. Even though research on numerical models has been ongoing for years, the present ribcage models still need some modifications and improvements, e.g. in terms of the rib cortical bone thickness distribution [11]. Usually they are developed from computed tomography (CT) images. Most of them are based on the full body clinical-CT which provides poor resolution (0.2 – 1 mm/voxel) and could result in a significant geometrical inaccuracy. However, clinical-CT offers a large field of view (FoV) and is a suitable method for living human subjects. Conversely, the micro-CT offers much better resolution (0.02 mm/voxel) but has limited FoV that does not allow full body scans. The micro-CT is suitable only for the PMHS and provides an opportunity to scan body parts and short bone segments.

The main issue when developing rib geometry from the CT images is an estimation of the cortical area,

R. Perz is a PhD student in Mechanical Engineering, Warsaw University of Technology, Institute of Aeronautics and Applied Mechanics, Poland and Research Assistant in Biomechanics, University of Virginia Center for Applied Biomechanics, USA (+48 22 234 7512 or +1 434 296 7288, rperz@meil.pw.edu.pl). J. Toczyski is a PhD student in Mechanical Engineering, Warsaw University of Technology, Institute of Aeronautics and Applied Mechanics, Poland and a visiting scholar, University of Virginia Center for Applied Biomechanics, USA. M. Kindig is a Research Scientist, University of Virginia Center for Applied Biomechanics. D. Ito and S. Ejima, Japan Automotive Research Institute (JARI), Tsukuba, Japan. K. Kamiji and T. Yasuki, Japan Automobile Manufacturers Association (JAMA), Tokyo, Japan. Prof. J. Crandall is Director, Center for Applied Biomechanics, University of Virginia, USA. D. Subit (P.I. of the project) is a PhD and a Senior Scientist, University of Virginia Center for Applied Biomechanics, USA.

especially separating it from the trabecular part of the bone. The modalities of the cortical thickness in human ribs vary up to 75%, depending on position [12]. In some parts of the rib the thickness of the cortical bone drops below 1 mm which is equal to or even smaller than the clinical-CT resolution. The choice of the proper threshold parameters is crucial at this point. There are many schemes and setups of the thresholds that should separate the cortical bone from the other tissues but most of them still overestimate the cortical thickness which results in geometrical inaccuracy which then increases with the diminishing CT image resolution. Regular clinical-CT images are used to derive the FE models of the thorax, but no quantification of the error due to the use of this method has yet been done, and this is one of the goals of this study. The micro-CT is so far the best known method to investigate the bone structure and develop proper bone geometry. However, the shape and size of the human ribs do not allow for performing a whole bone scan using the micro-CT method. Each rib has to be cut into a few sections in order to be scanned. This results in additional issues to be resolved before combining the images to create a finite element (FE) model.

Therefore, the objective of this study was to investigate whether rib FE models could be improved by combining two imaging modalities and to introduce a new method of determining the distribution of rib properties. The aim was to prove that proper rib geometry can be obtained from the clinical-CT images when adding correction factors obtained from the local micro-CT measurements. To validate the method the numerical model was implemented and compared to the experimental results. At this point a lot of work has been done on material properties of the bones, including ribs [13-14]. In this study the authors focused on the geometrical properties and methods only. There is no investigation on the influence of material properties of the model on its response. Also, no comparison of the effect of the material properties and geometrical properties variations has been done. The material properties were assumed to be given and just adjusted within the range to give the best mechanical response.

II. METHODS

Experimental Testing

The twelve left ribs from one 59 year old male PMHS were extracted in accordance with ethical guidelines and research protocol approved by the Human Usage Review Panel and a University of Virginia institutional review board. Prior to testing, the specimen was screened for HIV and hepatitis, and pre-test x-rays and CT scans were checked for signs of pre-existing bone and joint pathology.

Prior to this study, the ribcage of this PMHS was removed and its stiffness was tested in the table-top test. During the experiment ribs 3, 4, 5 and 8 were broken. Rib 8 was broken in the medial region and was excluded from further investigation. The rest of the broken ribs were dismembered at 20 – 30 mm from the anterior end. Since there is the potting at the ends, this part of the rib is outside the loaded fragment. Additionally it is known that such a small length decrease does not influence the rib behavior much [15-16]. It was decided that those ribs would be used for the next part of the experiment.

Each rib to be tested was separated from the body by cutting off the costal cartilage at the costochondral junction near the sternum and thoracic vertebra. After extraction the intercostal musculature and any other soft tissues were removed from the cortical bones. Cleaned bones were scanned according to the clinical-CT protocol and then potted at the posterior and anterior ends. The potting was prepared to be the box-shaped solid made of polyurethane resin with 5 x 5 x 3 cm dimensions. The positioning was set to keep the axis in the same vertical plane. Once potting was prepared the anterior, medial and posterior points at the ribs were determined. The medial part of the bone was picked to be at the most lateral point of the rib. The anterior and posterior points of the rib were marked near to the pots. Those points are essential for the next step – cutting the slices. Fully prepared ribs were subjected to another clinical-CT scan to show the exact position of the potting.

The antero-posterior bending test up to the fracture was performed using a servo-hydraulic material test machine (Instron 887). Both ends of the rib were attached to the testing fixture by the two pin joints, where the posterior joint had only one degree of freedom (rotation) and anterior part had two degrees of freedom (vertical and rotation), (Fig. 1).

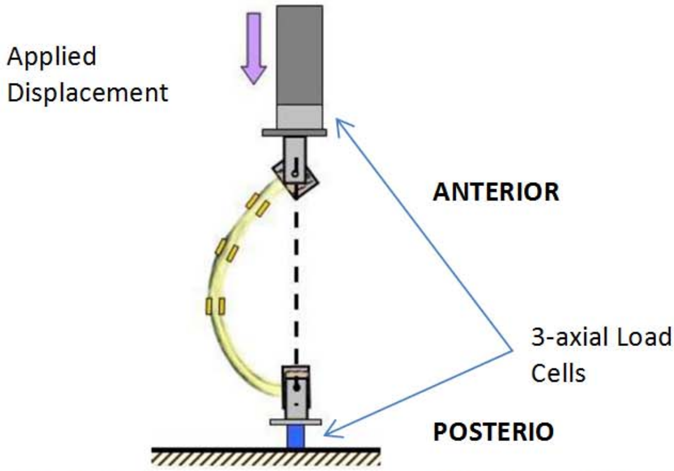

Fig. 1. The experimental setup with the instrumentation.

External instrumentation was used to measure the boundary condition response. It included two 3-axial load cells, one placed below the posterior potting and one placed above the anterior potting to check the response during loading. Also the string potentiometer was used to measure the displacement of the piston head. The data for the experiment were sampled with the 50 kHz frequency. The actuator piston speed for the experiment was constant and set to be 1 m/s.

Clinical-CT and Micro-CT Imaging

After the experimental bending test each rib was cut to obtain three 3-5 mm long sections (Fig. 2). The 1st and 12th ribs had only two slices due to the size. Each rib had slices from the anterior and posterior positions and ribs 2-11 had also medial slices giving 34 samples altogether. The positions of the slices were determined to be as close as possible to the previously determined positions. Once harvested the slices were placed in four custom designed containers to preserve their positions during micro-CT and clinical-CT.

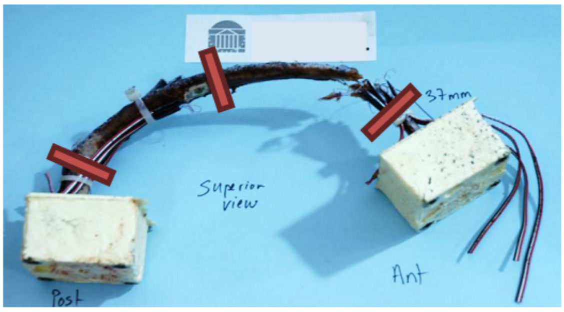

Fig. 2. An example of the rib section slice harvested from the medial part of the bone.

Two computed tomography imaging techniques were used during the study. Clinical-CTs were performed on the GE Optima CT660 Scanner [17] using two protocols: Regular Medical CT, with a resolution of 1 mm/voxel and 50 cm field of view (FoV) and High Resolution Medical CT (HRMCT), with a resolution of 0.373 mm/pixel, slice thickness of 0.625 mm and 19 cm FoV. Although the FoV of the first method gives the opportunity to perform full body scans, the resolution is insufficient for the ribs imaging purpose. Therefore, the HRMCT is a proper method for the whole rib scans and Regular Medical CT was not used for the further steps. The obtained images included the whole rib scans (ribs 3L, 4L and 5L) and the rib cross-section scans. The whole rib scans were used directly to evaluate the numerical model geometry, to determine the external surface and to screen the ribs for any preexisting fractures. The slices scans were used to compare the micro-CT and clinical-CT (HRMCT) and to determine the geometrical differences in the section geometrical properties.

The micro-CT scans were performed using a Scanco Medical µCT40 scanner [18]. The micro-CT offers resolution of 0.02 mm/voxel but the FoV is reduced to 4 cm diameter and 10 cm length. Because of the FoV this method is only suitable for small harvested samples. Since there is no better way to investigate the section geometrical and mechanical properties, the images obtained by that protocol are assumed to be the reference ones for the further comparison test.

Data Analysis

All the calculations based on the CT images were divided into two parts: the estimation of the clinical-CT geometry deviation and the presentation of the geometrical properties distribution along the rib. These involved evaluation of the cortical area, trabecular area, overall area, outer perimeter and two principal moments of inertia.

The geometry deviation points were developed from 34 slices that were scanned using Micro-CT and Clinical-CT protocols. The two sets of geometrical properties for each slice were obtained directly from the clinical-CT and micro-CT images using Mimics [19] and ImageJ [20] software and then compared with each other to obtain the percentage difference of the geometrical parameters.

The formula used to evaluate the deviations as a percentage difference between clinical-CT and micro-CT values is:

$$\frac{HRMCT\ val.\ -\ \mu CT\ val.}{\mu CT\ val.} \times 100\% \tag{1}$$

At the end, after obtaining values for each slice the average deviation values for each parameter were calculated. These average values were also used as correction values in further steps.

Development of Correction Functions

Once the deviations were obtained approximation functions were developed. These functions were used in the further steps as correction functions to adjust the reference properties distribution and the reference numerical models. The simplest method used was shifting results by the average deviation value. Then linear, 2[nd], 3[rd] degree polynomials and a power function were utilized. The aim was to check the influence of different approximation types on the given data and its sensitivity.

The correction algorithms were used only for the 15% to 85% rib length range. Both first and last parts were skipped due to the large shape irregularity and the fact that these parts were potted. Some of the developed functions result in a significant error at the ends of the ribs and do not work well there.

Processing Rib Geometry

The whole rib clinical-CT images were processed with the Mimics software to mask and evaluate the cortical part of the bones. This step involved developing precise rib geometry and transferring it to the numerical model. The cortical bone was exported as two surfaces (inner – trabecular and external – outer) to the Stereo Lithography (*.stl)* CAD files. Once the geometry was transferred to the CAD format it required minor "hand-cleaning" from noises and free particles. Then using a custom-built script the centroid was determined and the geometry was cut every 1% into one hundred slices (Fig. 3). Each slice plane was normal to the centroid at that point. The geometrical properties of each slice were extracted to find: cortical area, centroid position, principal moments of inertia and principal axes and then exported to the spread sheet and used for the further evaluation.

a) Rib and cutting planes b) Extracted slice outlines c) Extracted cortical surfaces

Fig. 3. Process of generating rib 5L beam model (example containing only 30 surfaces).

Computational Modeling

The last part of this study was to develop numerical models for the left ribs 3, 4 and 5. The goal was to create beam models that were fully adjustable (independently cortical area and moments of inertia) to evaluate how the parameter variations influence the mechanical response, to introduce the correction function in order to correct the response and to validate the numerical model results with the experiment.

The FE beam models were based on the obtained spread sheet files. The beam geometry was represented as the rib centroid. Each model contained one hundred connected elements with different areas, section orientation and moments of inertia. Such a model allows for changing each cross-sectional parameter separately and evaluating its influence on the stiffness and general mechanical behavior of the rib. The element formulation was picked to be *Belytschko – Schwer resultant beam* (ELFORM=2) with cross-section area and moments of inertia input. The bone material was modeled as elastic – perfectly plastic (without failure). Its properties were as follows: Young's modulus E = 11.5 GPa [21], Poisson's ratio υ = 0.3 and Yield stress σy = 98 MPa. The Young modulus and Poisson ratio were taken from the GHBMC model. The Yield stress was picked to give the best response results and to be consistent with the literature values [13-14]. The boundary conditions were prepared to exactly match the experiment. The exact position of the potting and the pin joints was included in the model development. Previous studies have shown that the difference between the quasi-static vs. dynamic response of a single rib (in terms of its stiffness) is not significant in a planar bending test performed at the loading rates of 0.5-1 m/s [15]. Due to this fact LS-Dyna R4.2.1 implicit code was used to carry out the simulations. In the end the results of the experiment, initial and corrected numerical models are compared.

III. RESULTS

Rib Cross-sections Comparison

The analysis of the images showed that the clinical-CT when compared to the micro-CT has a tendency to overestimate at average the cortical area, the overall area and the cortical area moments of inertia and underestimate the trabecular area (Table 1).

TABLE 1
GEOMETRICAL PROPERTIES DEVIATION RESULTS

Parameter	Min	Max	Mean	Std. Deviation
1st PMoI	20.6%	73.3%	49.7%	13.3%
2nd PMoI	19.2%	92.8%	56.8%	19.5%
Overall area	2.0%	13.7%	7.6%	2.9%
Cortical area	17.8%	66.9%	40.2%	12.5%
Trabecular area	1.7%	34.0%	13.3%	7.3%

The cause of such difference is the lower resolution of the clinical-CT. The pixel size of 0.373 mm is only slightly smaller than the cortical thickness in some points. This results in a blurred picture, where cortical thickness seems to be thicker than it really is (Fig. 4b). It may be noticed that the average overall area has the smallest deviation (7.6%). This is the effect of the sharp outer contour and lack of any tissues on that surface (Fig. 4).

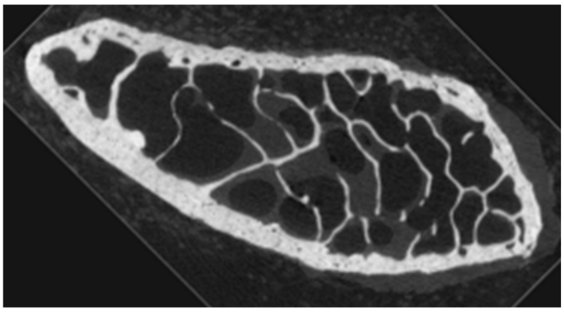

Fig. 4a. Example of the micro-CT image (10th rib, medial part)

Fig. 4b. Example of the corresponding clinical-CT image (10th rib, medial part)

On the other hand inside the bone the trabecular area has spongy structure with cortical-like particles. Since the images are in the grey scale, where white (cortical bone) is the maximum value and black (surrounding) is the minimum value, the trabecular part of the bone increases the average grey value. As a result the inner cortical contour is moved inside and the trabecular area is underestimated. This is also the reason why the cortical area and its moments of inertia are significantly overestimated. The deviation for the cortical part is a result of relocating out the outer contour and relocating in the inner contour – it doubles the deviation.

Beside the average deviations for each parameter, average deviations for each – anterior, medial, posterior – position were also presented (Tab. 2).

TABLE 2
PROPERTIES DEVIATION RESULTS FOR EACH POSITION ON THE RIB

Position	Anterior	Medial	Posterior
1st PMoI	53.9%	50.5%	45.7%
2nd PMoI	52.0%	65.9%	53.0%
Overall area	6.7%	10.2%	6.3%
Cortical area	40.4%	42.0%	37.6%
Trabecular area	14.3%	11.8%	15.5%

Geometrical Properties Distribution

The rib cross-section slices analysis allowed for determining several correction functions for changing the geometrical properties deviation along the rib (Fig. 5). The first and last 15% of the rib geometry were discarded because of the complex geometry and the presence of the potting (the rib changes its shape near the costochondral junction). It can be observed that all the functions result in a similar behavior. The functions were also checked with the distribution models to observe influence on the distribution trends.

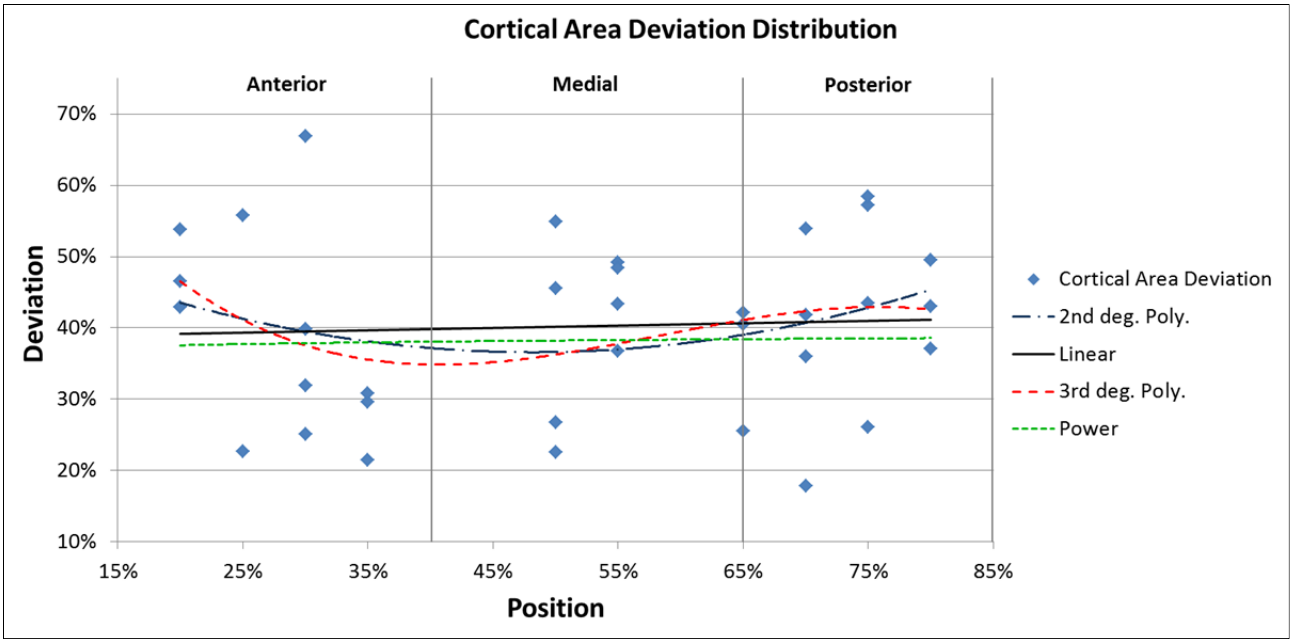

Fig. 5. The evaluation of the correction functions for the cortical area.

For the next step, the correction functions were applied to the rib model distributions (Figs. 6, 7, 8). The simplest correction function was shifting the cross-section parameters by the average deviation values. The values used were: 40.2% for the area, 49.7% for the first principal moment of inertia and 56.8% for the second principal moment of inertia.

It may be noticed that each function gives similar results and does not change the distribution trends or behavior. Hence, the average shifting correction seems to be the best choice as it gives very good results and is the easiest one to use. However, all the functions were used to check influence on the numerical model.

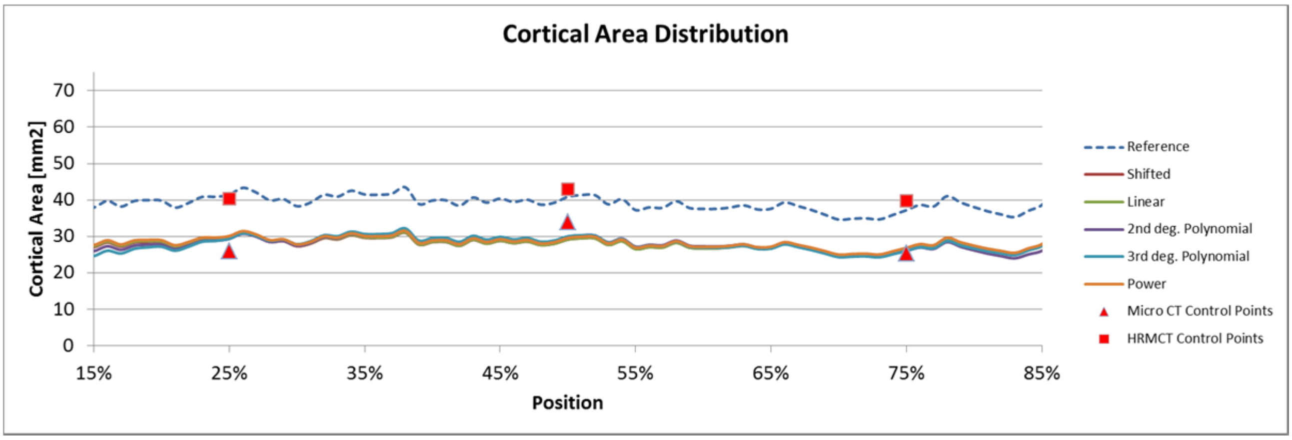

Fig. 6. The example of the properties distribution for the 5L rib when applying functions.

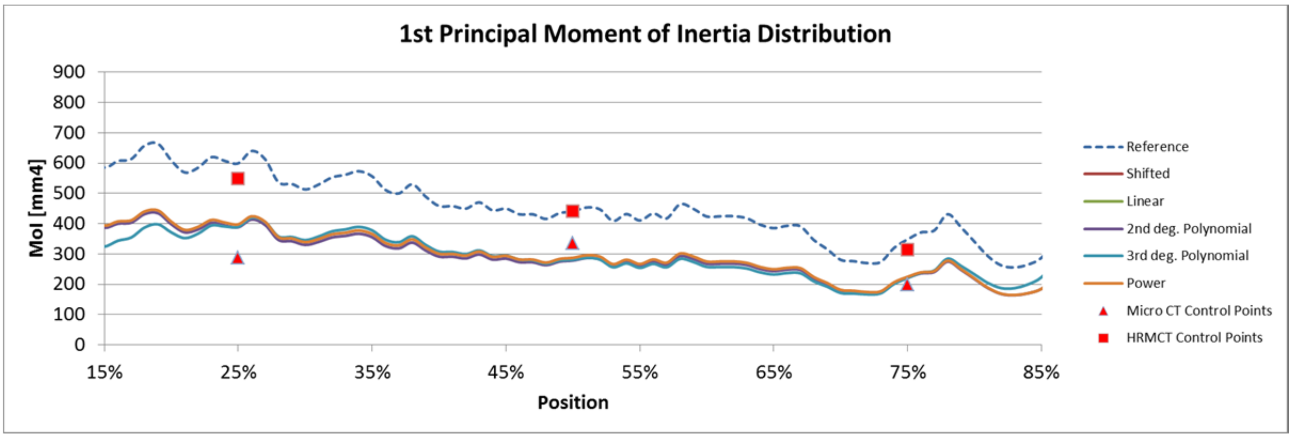

Fig. 7. The example of the properties distribution for the 5L rib when applying functions.

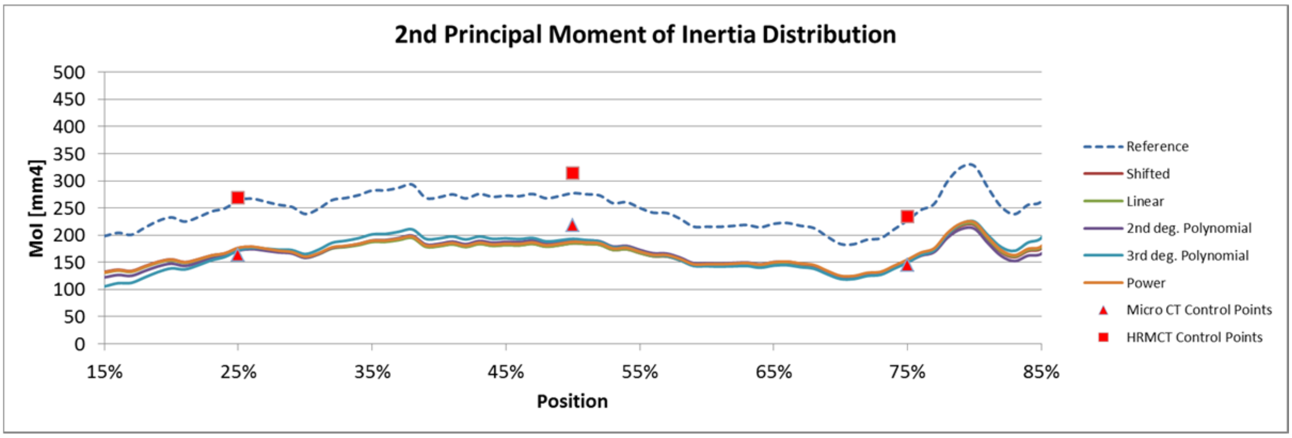

Fig. 8. The example of the properties distribution for the 5L rib when applying functions.

Computational Modeling Results and Experimental Data Comparison

At this stage used ribs were transferred to the beam element models using clinical-CT results. Once the beam geometry was evaluated, the geometry distribution correction functions were implemented to check the model modality and sensitivity for the changes in the geometrical properties.

The results showed that the response of the model was very sensitive to the moments of inertia change and significantly influenced the model's stiffness. The resultant force vs. displacement graph has been presented to illustrate the model's sensitivity and to show the influence of the correction functions on the model's behavior (Fig. 9).

The results from the corrected numerical models and experimental tests were compared to check the force vs. displacement response. The comparison to the experiment showed that any function used to correct numerical models gave very good and comparable results. The model's behavior was similar to the experimental results. The stiffness of the numerical ribs was almost the same as the stiffness of the real bone. That suggests the model was developed correctly and correction functions gave reliable results.

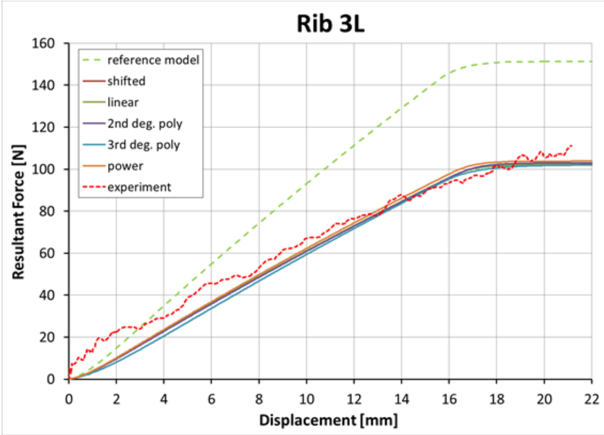

a)

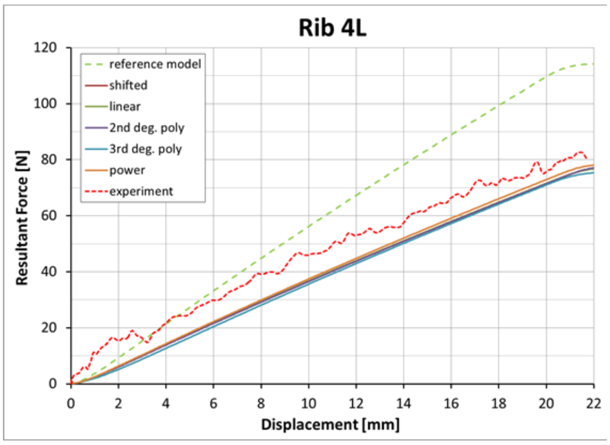

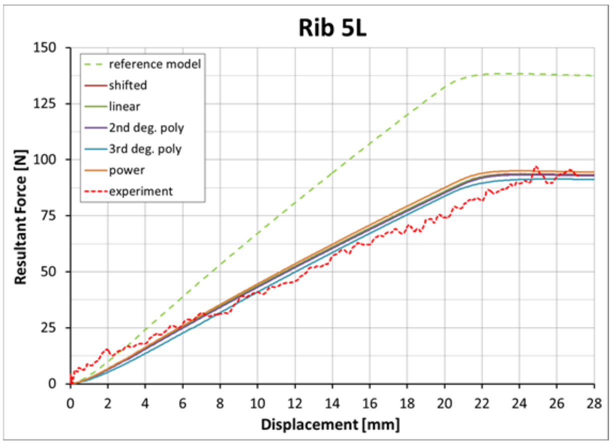

b) b)

Fig. 9. The numerical model responses compared to the experimental results

IV. Discussion

So far the rib models have been mainly represented as the solid (trabecular part)-shell (cortical part) body models with the average cortical bone thickness applied [22-23]. Beam models have also been developed, but again the initial point for the simulations was the surface with the averaged cortical thickness. The method described in the paper presents a different approach where the full 3D, double surface limited geometry from X-ray imaging is implemented in the beginning. Then the solid, cortical part of the bone is cut for the slices and each slice presents the cortical surface instead of the mid-surface perimeter with the cortical thickness applied to it. Although the presented method is much more time consuming, it gives accurate results and is the most appropriate way to develop a universal solution to scale the clinical-CT ribs geometry, to remove the deviations and to obtain the accurate geometry that would give the proper FE model response. While analyzing the results, it was observed that deviation depends on the slice size. However, the size of the slices does not vary much among the ribs along similar locations [12]. Therefore it was assumed that function could be fitted with respect to a position along the rib (Fig. 5).

The beam model used in this study has a distinct advantage over the 3D solid/solid-shell models. Unlike them it can be fully adjusted for any parameter using even complicated functions and the entire process can be done within minutes. However, it was shown that all the proposed correction methods give similar results so it would be almost impossible to check with the use of the solid model. The disadvantage of the beam model is poor implementation of plasticity and damage prediction. This means that the beam model would not support the estimation of the injury criterion. Also it is not possible to analyze the stress-strain results. This raises the issue of the significance of the cortical area and moments of inertia. It would not be incorrect to say that moments of inertia are more important than area in this particular case. The rib is subjected to antero-posterior bending where bending stiffness plays a key role. The moments of inertia are directly responsible for the stiffness and the cortical area (along with moments of inertia) mostly influences the yield strength. It means that the rib slice projection is very important in the model development.

The investigation of the material properties' influence on the model was intentionally skipped. The responses of the beam element models of the ribs 3rd -5th fit the experimental data well (Fig. 9). The results were much improved by modifying only the geometric parameters (MoI and cortical area). If the variation of material properties was added to the study, the effect of mesh density, element formulation, etc. should also be investigated, as shown in [11] but that was not the part of the study.

The greatest variable in this study was the CT images processing. There are many available threshold methods, but still the biggest issue was the export of the cortical part of the bone. Mainly this problem was related to the small cortical bone thickness. As mentioned before, in some parts of the rib cortical thickness decreases to the size of the pixel. This means that an inaccurately picked threshold method could change the geometric parameters considerably. For example, if the threshold overestimates the rib slices area and adds one extra layer of pixels (0.3 mm/pix) outside the perimeter, then for the average-size slice (area = 75 mm^2 and perimeter = 35 mm) the area could be increased by 10 mm^2 which results in 13.3% deviation. It also influences the moments of inertia – one additional layer of pixels changes the relative width and length of the rib slice. This shows the importance of the proper threshold. Especially problematic was the trabecular area separation which is relatively small and contains weighty parts of cortical tissue inside. This causes the inner area of the trabecular bone image to be a light gray. Near the cortical bone it is even lighter, almost white, and that makes the threshold script separate cortical and trabecular areas incorrectly. Even though present threshold methods give very good results with the larger bones, their effect with the ribs still remains uncertain. Also, the export procedure could influence the final output. Creating the mesh surface from the pixel ribs could run in unwanted directions. The offered exporting parameters variety could completely change the rib model parameters.

An important consideration with the proposed method is the time-consuming process to extract the exact geometry of the rib body. The process requires a lot of attention and hand correction as described in this paper. However, all the data were based only on clinical-CT. This means that with a little more effort there would be no need to scan the body with the micro-CT protocol. With the proper correction functions the clinical-CT would be enough to represent the human thorax model. As a consequence, human chest models can be developed since clinical-CT and its FoV are suitable to use with living humans.

This study is still ongoing. There is still a need to improve the function so it would work for the entire length of the rib. So far only three full rib models have been created, converted and checked. It is necessary to carry out the analysis on the ribs obtained from other PMHS. This would confirm that the method is universal and can be applied for every specimen. The plan is to analyze the ribs from other specimens to check the correction values for them. It is yet unknown what would be the result of applying this method to the 5th percentile female or 95th percentile male. Since the quality of the clinical-CT images highly depends on the cortical bone size, the correction functions and the results might be slightly different for those specimens. There is a need to check that trend.

Another possibility would be to see if this method might be applicable for the whole ribcage model. The human thorax, in addition to the bare ribs, consists of the cartilage tissues, muscles, etc. that might influence the final response. Especially interesting would be the influence of the costochondral junction area.

V. CONCLUSIONS

This study reports on a method to evaluate the rib geometrical properties distribution using a combination of clinical-CT and micro-CT images. This combined approach is necessary because, on the one hand, clinical-CT rib scans do not allow representation of the proper rib geometry due to the low resolution. On the other hand, it is not possible to scan whole ribs using only micro-CT scan because of the limited field of view. It has been shown that by using only several control points from the micro-CT images we are able to introduce the correction function for the rib geometry. Combining clinical-CT distribution with the presented functions gives the improved properties distribution curve. Such a curve when used to implement the numerical beam model gives a response that is similar to the experimental results for the respective ribs and proves that the method works as intended.

VI. ACKNOWLEDGEMENTS

The research (experimental work and X-ray imaging) was sponsored by the Japan Automobile Research Institute (JARI). The study presented in the article was also supported in part by the European Union in the framework of European Social Fund through the "Didactic Development Program of the Faculty of Power and Aeronautical Engineering of the Warsaw University of Technology."

The authors would like to thank the Materialise Company for the support with the Mimics software license.

VII. REFERENCES

[1] Foret-Bruno JY, Trosseille X, Page Y, Huere JF, LeCoz JY,Bendjellal F, Diboine A, Phalempin T, Villeforceix D, Baudrit P. Guillemot H, Coltat JC, Comparison of thoracic injury risk in frontal car crashes for occupant restrained without belt load limiters and those restrained with 6 kN and 4 kN belt load limiters, *Stapp Car Crash Journal,* 45:205-24¸2001.

[2] Nahum A and Melvin J, (eds.), Accidental Injury – Biomechanics and Prevention, *Springer-Verlag,* New York, 1993.

[3] Mulligan GWN, Pizey G, Lane D, Andersson L, English C, Kohut C, An introduction to the understanding of blunt chest trauma, In: Biomechanics of Impact Injury and Injury Tolerances of the Thorax-Shoulder Complex, *Society of Automotive Engineers* publication PT-45, 1994.

[4] Malliaris AC et al., Harm causation and ranking in car crashes, *Society of Automotive Engineers,* paper No. 850090, 1985.

[5] Salzar RS, Lau SH, Lessley DJ, Sochor MR, Shaw CG, Kent RW, Crandall JR, Thoracic response to shoulder belt loading: comparison of tabletop and frontal sled tests with PMHS, *Traffic Injury Prevention,* 143(2):159-67, 2013. Kimpara H, Lee J, Yang K, King A, Iwamoto M, Watanabe I, Miki K, Development of a three-dimensional finite element chest model for the 5th percentile female, *Stapp Car Crash Journal,* 49:251-269, 2005.

[6] King M, Zuoping L, Kent R, Subit D, Effect of intercostal muscle and costovertebral joint material properties on human ribcage stiffness and kinematics, *Computer Methods in Biomechanics and Biomedical Engineering*, under review.

[7] Lizee E, Robin S, Song E, Bertholon N, Le Coz, J, Besnault B, Lavaste F, Development of a 3d Finite Element Model of the Human Body, *42nd Stapp Car Crash Conference Proceedings*, 1998.

[8] Robin S, Human model for safety: a joint effort towards the development of refined human-like car occupant models, *Proceedings of the 17th International Technical Conference on the Enhanced Safety Vehicle,* Paper 297, 2001.

[9] Shigeta K, Kitagawa Y, Yasuki T, Development of next generation human finite element model capable of organ injury prediction, *Proceedings 21st ESV Conference*, Paper 09-0111, 2009.

[10] Song E, Trosseill X, Baudrit P, Evaluation of thoracic deflection as an injury criterion for side impact using a finite elements thorax model, *Stapp Car Crash Journal,* 53: 155-91, 2009

[11] Li Z, Kindig MW, Subit D, Kent RW, Influence of mesh density, cortical thickness and material properties on human rib fracture prediction, *Medical Engineering & Physics*, 32(9):998-1008, 2010.

[12] Mohr M, Abrams E, Engel C, Long WB, Bottlang M, Geometry of human ribs pertinent to orthopedic chest-wall reconstruction*, Journal of Biomechanics*, 40:1310-1317, 2007.

[13] Kemper AR, McNally C, Kennedy EA, Manoogian SJ, Rath AL, Ng TP, Stitzel JD, Smith EP, Duma SM, Matsuoka F, Material properties of human rib cortical bone from dynamic tension coupon testing, *Stapp Car Crash Journal*, 49:199-230, 2005.

[14] Subit D, del Pozo de Dios E, Valazquez-Ameijide J, Arregui-Dalmases C, Crandall J, Tensile material properties of human rib cortical bone under quasi-static and dynamic failure loading and influence of the bone microstucture on failure characteristics, arXiv:1108.0390v2 [physics.bio-ph], 2011.

[15] Kindig M, Tolerance to failure and geometric influences on the stiffness of human ribs under anterior-posterior loading, *M.Sc. dissertation, University of Virginia, School of Engineering and Applied Science*, 2009.

[16] Li Z, Kindig M, Kerrigan JW, Untariou CD, Subit D, Crandall JR, Kent RW, Rib fractures under anterior-posterior dynamic loads: experimental and finite element study, *Journal of Biomechanics*, 43(2):228-234, 2010.

[17] GE Healthcare – Optima CT660 – Internet: [www.gehealthcare.com], 2013.

[18] Scanco Medical – uCT 40 – Internet: [www.scanco.ch], 2013.
[19] Mimics software, Internet: [http://biomedical.materialise.com/mimics], 2013.
[20] Schneider CA, Rasband WS, Eliceiri KW, NIH Image to ImageJ: 25 years of image analysis, *Nature Methods,* 9: 671-675, 2012.
[21] Gayzik FS, Moreno DP, Vavalle NA, Rhyne AC, Stitzel JD, Development and Validation of a Novel Full Human Body Finite Element Model Utilizing a Multi-Modality Medical Imaging Protocol, *ICRASH Proceedings*, 2012.
[22] Choi HY, Kwak DS, Morphologic characteristics of Korean eldery rib, *Journal of Automotive Safety and Energy*, 2(2):122-127, 2011.
[23] Choi HY, Thorax FE model for older population, *Hongik University, Inhyeok Lee, ESI,* Korea, 2000.